

Development of surface pattern during division in *Paramecium*

II. Defective spatial control in the mutant *kin241*

MARIA JERKA-DZIADOSZ^{1,2}, NICOLE GARREAU DE LOUBRESSE¹ and JANINE BEISSON^{1,*}

¹Centre de Génétique Moléculaire, Centre National de la Recherche Scientifique, 91198 Gif-sur-Yvette, France

²Department of Cell Biology, M Nencki Institute of Experimental Biology, Polish Academy of Sciences, 02-093 Warsaw, Poland

*Author for correspondence

Summary

kin241 is a monogenic nuclear recessive mutation producing highly pleiotropic effects on cell size and shape, generation time, thermosensitivity, nuclear reorganization and cortical organization. We have analyzed the nature of the cortical disorders and their development during division, using various specific antibodies labelling either one of the cortical cytoskeleton components, as was previously done for analysis of cortical pattern formation in the wild type.

Several abnormalities in basal body properties were consistently observed, although with a variable frequency: extra microtubules in either the triplets or in the lumen; nucleation of a second kinetodesmal fiber; abnormal orientation of the newly formed basal body with respect to the mother one. The latter effect seems to account for the major observed cortical disorders (reversal, intercalation of supplementary ciliary rows).

The second major effect of the mutation concerns the spatiotemporal map of cortical reorganization during division. Excess basal body proliferation occurs and is correlated with modified boundaries of some of the cortical domains identified in the wild type on the basis of their basal body duplication pattern.

This is the first mutant described in a ciliate in which both the structure and duplication of basal bodies and the body plan are affected. The data support the conclusion that the mutation does not alter the nature of the morphogenetic signal(s) which pervade the dividing cell, nor the competence of cytoskeletal structures to respond to signalling, but affects the local interpretation of the signals.

Key words: *Paramecium*, *kin241*, cortex, basal body, morphogenesis.

Introduction

The cortical pattern of *Paramecium* is determined by the arrangement of the ciliary basal bodies and their associated cytoskeletal structures and networks which delineate several thousand juxtaposed unit territories, the cortical units. These units are each centered around one (or two) basal bodies, are polarized and tandemly aligned in longitudinal adjacent rows (Ehret and McArdle, 1974; Allen, 1971; Sonneborn, 1970). At the whole cell level, this repetitive organization is tailored into an asymmetrical and polarized pattern whose center of asymmetry is the oral apparatus (a funnel-shaped organellar complex for food capture and phagocytosis) located in the middle of the ventral surface. As *paramecia* multiply by binary fission along an equatorial furrow, their division requires complex morphogenetic processes with duplication of the oral apparatus and reconstruction of the cortical pattern in the two daughter cells, respectively, developing from the anterior and posterior halves of the mother cell.

Pattern development during division in wild-type

Paramecium has been analyzed using immunological probes specific for each of the major components of the cortical cytoskeleton, whose individual spatiotemporal map of duplication/reorganization was established (Iftode et al., 1989). That study demonstrated the existence of morphogenetic signal(s) progressing over the dividing cell as wave(s) originating from the oral apparatus and the fission furrow, and triggering the duplication or reorganization of the different cortical structures and networks. Most importantly, that study also showed that, despite their similar organization, cortical units do not all respond in the same way to the morphogenetic waves and as a consequence do not contribute equally to the overall doubling of their number. The individual response of units depends on their position, the cortex being composed of several domains of differential morphogenetic potential. What is the nature of the morphogenetic potential? What is the nature of the morphogenetic signals that pervade the cell and how do they propagate? What is the structural and/or biochemical basis of domain differentiation? What is the relationship between the local

control of basal body duplication, known to be constrained within each cortical unit (Beisson and Sonneborn, 1965; Dippell, 1968) and the global control of basal body proliferation? One way to address these questions is to study mutations affecting cortical morphogenesis.

Several mutants characterized by cortical disorders and abnormal cell shape had been previously isolated (Beisson and Rossignol, unpublished data). The immunocytological dissection of pattern formation in the wild type (Iftode et al., 1989) provided a method and reference for the analysis of the morphogenetic defects in these mutants. We present here the study of one of them, *kin241* (Beisson et al., 1976). We show that in contrast to all previously reported mutations affecting cortical pattern in ciliates (reviewed by Jerka-Dziadosz and Beisson, 1990), this monogenic recessive nuclear mutation affects both cortical unit organization and polarity and global pattern. It causes mispositioning of newly formed basal bodies and modifies the contour and morphogenetic potential of some cortical domains. The contributions of this analysis to our understanding of morphogenetic processes in *Paramecium* and the possible molecular basis of the mutational defects are discussed.

Materials and methods

Strains, crosses and growth conditions

The strains used were the wild-type (*wt*) strain *d4-2* of *Paramecium tetraurelia*, a derivative of stock 51 (Sonneborn, 1974) and the mutant *kin241* obtained by UV mutagenesis of stock *d4-2*, characterized in particular by a larger cell size and cortical disorders (Beisson et al., 1976).

In order to analyse the progressive expression of the mutation, crosses between *kin241* and wild-type were carried out according to standard protocols (Sonneborn, 1975) and after autogamy of the F_1 *kin241/kin241*⁺ heterozygotes, homozygotes *kin241/kin241* were recovered from the wild type cytoplasmic F_1 line. The mutant homozygotes were identified by the second division following autogamy on the basis of their thermosensitivity, as *kin241* cells die within 24 hours at 35°C. Selected F_2 mutant lines were thereafter maintained by daily subcloning and their age in number of postautogamy divisions recorded.

Cells were grown at 27°C (or at 35°C for the above mentioned thermosensitivity test) in buffered Wheat Grass Powder (Pines International Co., USA) infusion containing 0.4 µg/ml β-sitosterol and bacterized the day before use with *Klebsiella pneumoniae*.

Immunofluorescence

Immunolabelling was performed as previously described (Iftode et al., 1989). Cells were permeabilized in PHEM buffer (Schliwa and Van Blerkom, 1981) containing 1% Triton X-100 for 5-10 minutes and incubated 1 hour at room temperature in the primary antibody. The cells were then washed three times in PHEM buffer containing 3% bovine serum albumin and 0.1% Tween-20, incubated 1 hour in the secondary antibody (FITC-labelled goat anti-rabbit antibody or sheep anti-mouse IgG antibody (both from Pasteur Production, Paris), washed twice and mounted in Citifluor (London).

Antibodies

The microtubular structures were visualized by a rabbit antiserum raised against *Paramecium* axonemal tubulin (Cohen et al., 1982). The cells were deciliated by two successive transfers into 2% MnCl₂ for 5 minutes (Fukushi and Hiwatashi, 1970) before permeabilization and incubation in the serum. The kinetodesmal fibers (striated ciliary rootlets, cr) were labelled by a rabbit antiserum raised against the paramecium purified structure (Sperling et al., 1991). Epiplasm (Iftode et al., 1989; Keryer et al., 1990) was labelled by the monoclonal antibody *CTR211*, kindly provided by Bornens, obtained from a library of antibodies raised against human centrosomes (Bailly et al., 1988; Bornens et al., 1987). The infraciliary lattice (Garreau de Loubresse et al., 1988; 1991) was labelled by the anti-EEB (Ecto-Endoplasmic Boundary), a rabbit antiserum raised against the EEB of *Isotricha* (Viguès and Grolière, 1985). In some experiments, double labelling involving anti-tubulin and anti-cr or *CTR211* and anti-cr was used.

The polyclonal antibodies were diluted 1/400 and the monoclonal antibody was used as culture supernatant diluted 1/2 in PHEM buffer containing 3% BSA and 0.1% Tween-20.

Electron microscopy

Cells were fixed for 1 hour in 2% glutaraldehyde at 4°C in cacodylate buffer 0.05 M, pH 7.2. After washing in the same buffer, the cells were postfixed in 1% osmium tetroxide in cacodylate buffer. Some samples were fixed in a freshly made direct mixture containing 1.5% glutaraldehyde and 1% osmic acid buffered with the cacodylate buffer for 1 hour at 4°C. Samples were then washed, dehydrated by passage through a series of alcohols and propylene oxide, before being embedded in Epon. Thin sections were contrasted with alcoholic uranyl acetate and lead citrate, then examined with a JEM 1200 EX or a Philips E M 201.

Results

The mutation *kin241* displays highly pleiotropic effects yielding larger cell size with an elongated and often bent anterior part, increased generation time (approx. 8 hours at 27°C as compared to 5 hours for the wild type), thermosensitivity (cells die within 24 hours at 35°C), cortical disorder and abnormal nuclear reorganization (Beisson et al., 1976). All these defects cosegregate as a single recessive Mendelian unit. The present study only concerns the effects of the mutation on cortical organization and morphogenesis. The cortical pattern was analyzed in both interphase and dividing mutant cells by immunofluorescence and electron microscopy. Because cortical disorders, even when accidental, can generate longterm inherited abnormalities, such as inverted ciliary rows (IR), which complicate the analysis of the direct effects of the mutation, studies were carried out on two types of mutant lines: established ones and 'new' lines, i.e. newly formed homozygous *kin241/kin241* F_2 clones derived from the wild-type cytoplasmic parent from *kin241* × wild-type crosses, in which the early expression and cumulative effects of the mutation could be monitored from 3-5 to over 70 cell generations after acquisition of the homozygous mutant genotype. Whether in new or established lines, a large variability in cell size or shape

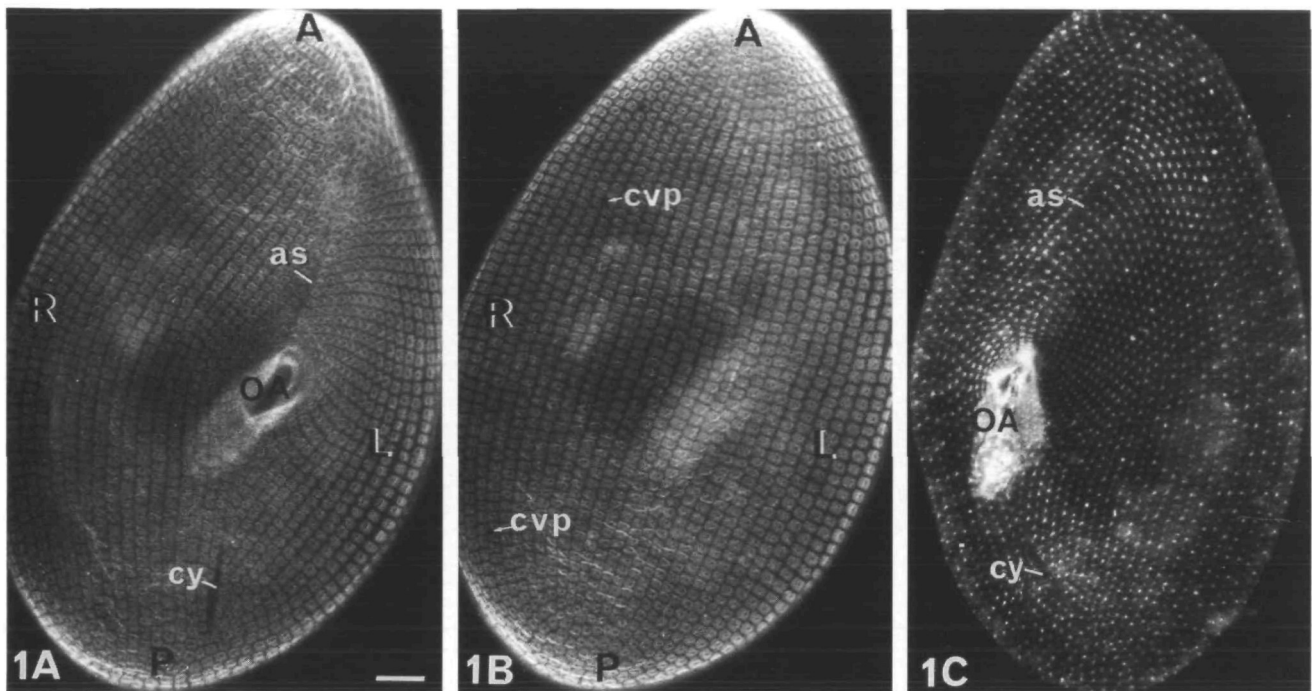


Fig. 1. Cortical organization in interphase wt cells revealed by immunostaining of epiplasm (A,B) and basal bodies (C). Ventral (A) and dorsal (B) sides of the same cell. The monoclonal CTR211 stains scale-like territories that correspond to cortical units. Holes in the centre of units correspond to the site of insertion of basal bodies. OA, oral apparatus; as, anterior suture; cvp, contractile vacuole pores, cy, cytoproct. A, P, R, L, respectively anterior, posterior, right and left of the cell. (C) Ventral side of another cell stained with anti-tubulin antibody $\times 680$; bar, $10\ \mu\text{m}$

and in the extent of cortical disorders is observed within growing populations and even intraclonally. Despite this variability, a typical *kin241* phenotype can be defined.

(I) Interphase organization

Figs 1 A-C and 2 A-C respectively show the wild-type and mutant cortical patterns as revealed by decoration with two different antibodies: CTR 211, which stains the epiplasm and visualizes the cortical units (cus) in which one or two basal bodies are anchored (A, B), and anti-tubulin antibodies, which stain the basal bodies (C). In addition to different size, shape and proportions (relative lengths of the body parts anterior and posterior to the oral apparatus; OA), a number of gross abnormalities are visible in the mutant: severe disorders in the arrangement of cus on the right side of the anterior suture; incomplete ciliary rows not extending from pole to pole or from anterior to posterior suture (Fig. 2B, arrows); a smaller size of cus with less regular shape and alignment; an increased number of contractile vacuole pores on the dorsal side (not shown). Another characteristic feature of the wild-type pattern is modified in the mutant: the regular organization of the left anterior half of the ventral surface in which cus are in register in both longitudinal and lateral directions, is restricted in the mutant to a smaller area near the anterior suture. This defect is correlated with a more subtle change in the basal body pattern. In wild-type cells, units with either 1 or 2 basal bodies (1-bb vs

2-bb units) are distributed in defined domains (Sonneborn, 1975; Iftode et al., 1989) as shown in Fig. 3A. The modified extension of these domains in the mutant is shown in Fig. 3B, which summarizes observation of many cells such as those presented in Fig. 2C.

Immunodecoration by the anti-ciliary rootlet serum revealed abnormalities in their orientation. In wild-type cells, ciliary rootlets (crs) are nucleated on the right side of basal bodies and point towards the anterior cell pole. Along each ciliary row, they intertwine with the 1-3 anterior ones and form a rope-like structure, which parallels the alignment of basal bodies along each longitudinal row. In the mutant, two types of abnormalities are consistently observed: patches of severe disorders where crs run in all directions (Figs 4A, 5A, B) and patches of inverted rows (IR) in which the cr polarity is 180° reversed (Fig. 4B). Additional defects visible at the ultrastructural level are present: abnormal organization of the crs (Fig. 5B) and abnormal organization of ciliary structures with supernumerary microtubules (Fig. 5C).

The disorders expressed in basal body, cu and cr arrangement extend to the innermost cytoskeletal network, the infraciliary lattice (Fig. 6) whose meshes run around the proximal end of basal bodies. The contours of the meshes are much more irregular in the mutant. In particular, the anterior suture is not well defined. Altogether it appears that all the cortical cytoskeletal structures show spatially correlated disorders.

Quantitative data on new (25-33 division old) and

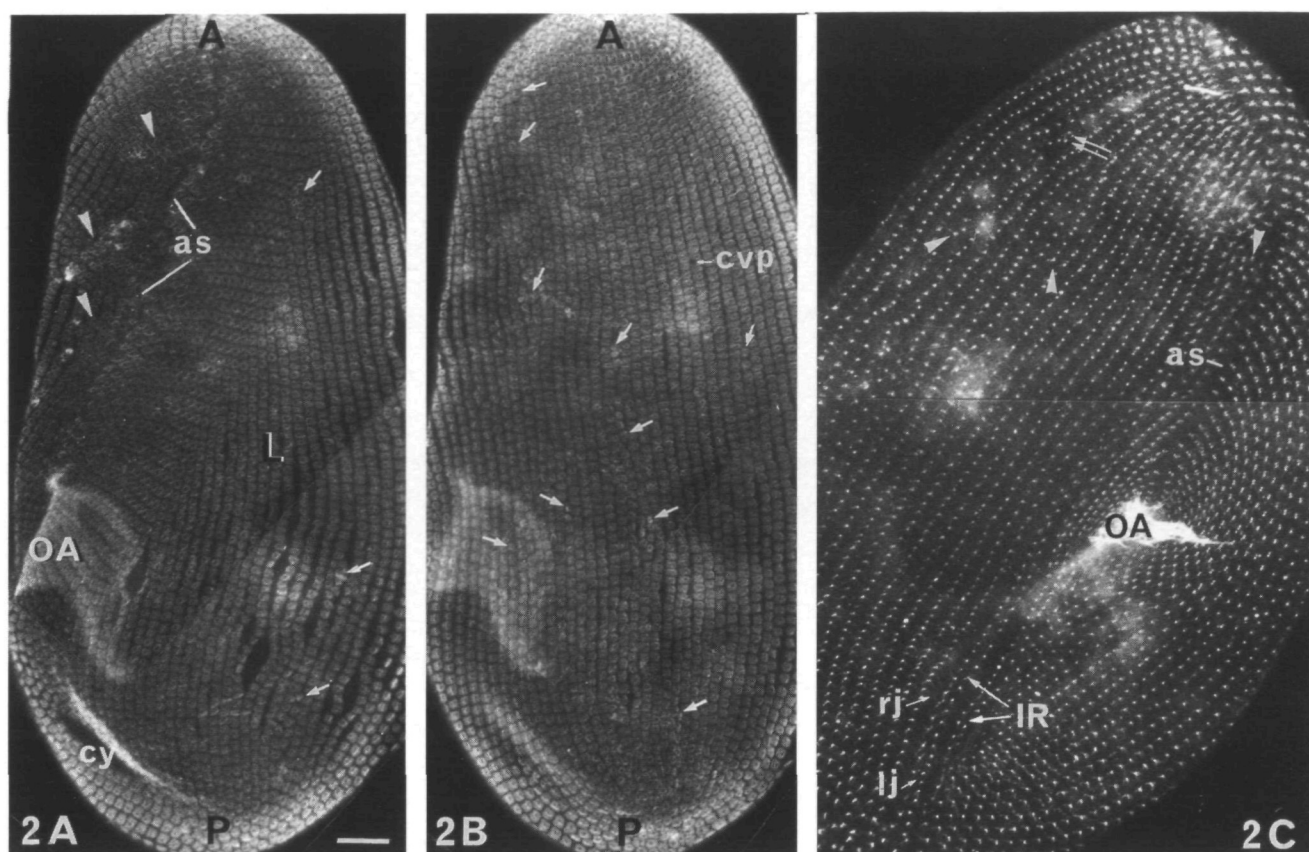


Fig. 2. Cortical organization in interphase *kin241* cells revealed by immunostaining of epiplasm (A, B) and basal bodies (C) (A) Left ventral view. Note the long and irregular anterior suture (*as*) and three groups of irregular patches of units at the right side of the suture (arrowheads). Small arrows point to ends of rows of units on ventral and dorsal (B) sides. The left dorsal sector shows the most regular pattern. On the right side of the images the files of units are slightly disrupted as a result of compression between slide and coverslip. (C) In addition to basal bodies, remaining cilia in the OA are stained and short postciliary and transverse microtubule ribbons attached to basal bodies are visible especially around the posterior pole. *IR*, inverted rows of basal bodies. Note the larger spacing between rows at the right juncture (*rj*) and close apposition at the left juncture (*lj*). Arrowheads point to ends of short ciliary rows. The double arrow indicates a sector with erratic basal bodies $\times 680$; bar, 10 μm .

established mutant lines concerning cell size, number and size of cus, 1-bb:2-bb unit ratio, number of ciliary rows, number and position of contractile vacuole pores (cvps) and inverted rows (IR), number of ciliary rows abutting on the anterior suture are presented in Table 1 and Fig. 7. It can first be noted that the cell size and number of ciliary rows, cus, cvps are smaller in the new lines after approximately 30 divisions than in the established lines whose characteristic phenotype is acquired progressively and reaches a steady state after about 75 divisions. Secondly, it appears that supernumerary ciliary rows are not distributed at random. Table 1 and Fig. 7 show that their number equals that of the rows added on the left ventral side. This accounts for the elongated anterior part of the cell and possibly for the disorders observed on the right side of the anterior suture. Thirdly, the 2-bb:1-bb ratio is reduced in the mutant, in agreement with the previously noted alteration of their respective domains (Fig. 3B). Finally, the first complete IR were observed in new

lines after about 30 divisions. In established lines, their localization is not random. They most frequently occur in sectors corresponding to 5-10% and 30-45% of the cell circumference (Figs 2C, 4A, B) as measured from the oral meridian toward the right. In very young clones, IRs were observed on the left ventral side but seemed to be unstable.

According to previous studies (Beisson and Sonneborn, 1965), IR most likely originate from erratic bbs whose polarity happens to be 180° rotated and whose duplication can generate IRs eventually extending from pole to pole. The existence in wild-type cells of a slow migration ('cortical slippage') of ciliary rows from right to left has been documented (Beisson and Sonneborn, 1965; Iftode and Adoutte, 1991). In the mutant, the prevailing occurrence of IR to the right half of the cell circumference would suggest that either basal bodies of erratic polarity are more likely to be produced on the right of the cell and/or that cortical slippage does not proceed as in wild type.

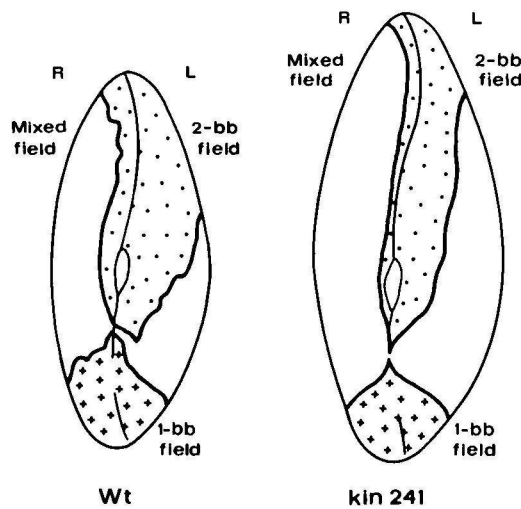


Fig. 3. Regional differentiations in the cortical pattern. Cortical units may contain either one or two basal bodies. As first noted by Sonneborn (1975), the distribution of the two types of units (1-bb vs 2-bb) is regionalized, on the ventral surface, into 3 fields: 1-bb unit only (crosses); 2-bb units only (dots); mixed 1-bb and 2-bb units (blank), as shown on the left for the wild type (redrawn from Fig. 6 of Iftode et al., 1989). In *kin241*, the regionalization is preserved but the contours and relative extension of the fields are modified.

(II) Cortical morphogenesis during division

Reorganization and duplication of cortical structures were examined on dividing mutant cells and compared to the processes described for wild type (Iftode et al., 1989). Globally, division in *kin241* proceeds normally as far as duplication of the oral apparatus, separation of the old and new ones and their coupling with nuclear division, cortical elongation and furrowing are concerned. Furthermore, despite a much longer generation time, division in the mutant lasts about the same time (about 20 minutes) as in wild type (although sometimes with a delay in the final separation of the daughter cells) so that stage-by-stage comparison of dividing cells in mutant and wild type is possible. With variable expression from cell to cell, alterations in both the spatiotemporal progression of morphogenetic events and in the reorganization of ciliary units were observed.

(A) Alterations in the spatiotemporal map of cortical morphogenesis

For the sake of clarity, a schematic overview of the early progression of the wave of cortical reorganization in wild type and mutant is presented in Fig. 8.

Basal body proliferation starts, as in wild type, in the left and right vestibular rows and along an equatorial belt over 4-5 cus posterior to the fission line. Slightly later, the cytoskeleton appears over the same regions and will progress first as discontinuous patches throughout

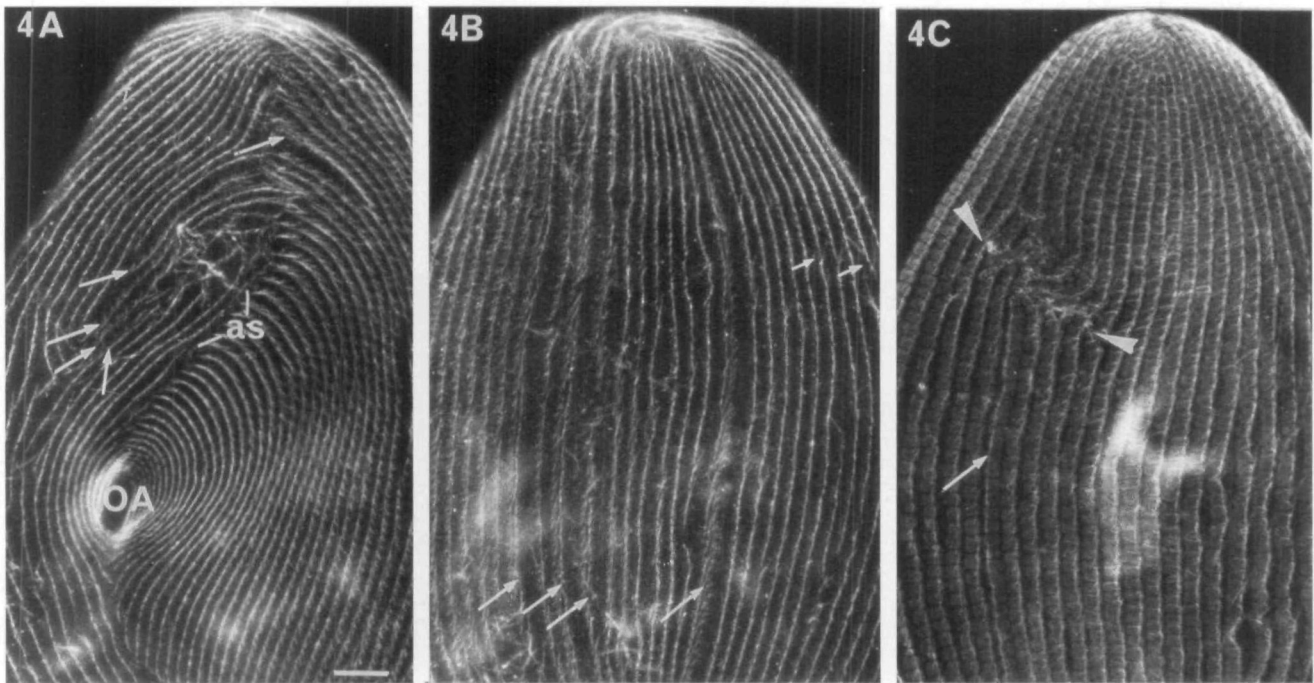


Fig. 4. Visualization of ciliary rootlets (kinetodesmal fibers) in *kin241* cells. Cells were immunodecorated either by the anti-ciliary rootlet antibodies (A, B), or double labelled by the anti-ciliary rootlet and the anti-epiplasm antibodies (C). Ciliary rootlets are nucleated on basal bodies and normally point to the right and anterior of the cell, while in inverted rows (IR) they point toward the left and posterior. A and B are the ventral and dorsal sides of the same cell. On the ventral side (A), 4 IR are present on the right of the anterior suture (as) and one on its left side (arrows); on the dorsal side (B), 4 IR are also visible (arrows). Small arrows point to the major disorders in ciliary rootlet orientation. (C) On another mutant cell, the double staining reveals a patch of disordered cortical units (arrowheads, with one IR posterior to the patch (arrow). The bright zone is due to the oral apparatus (OA) on the hidden side of the cell. $\times 680$; bar, 10 μm .

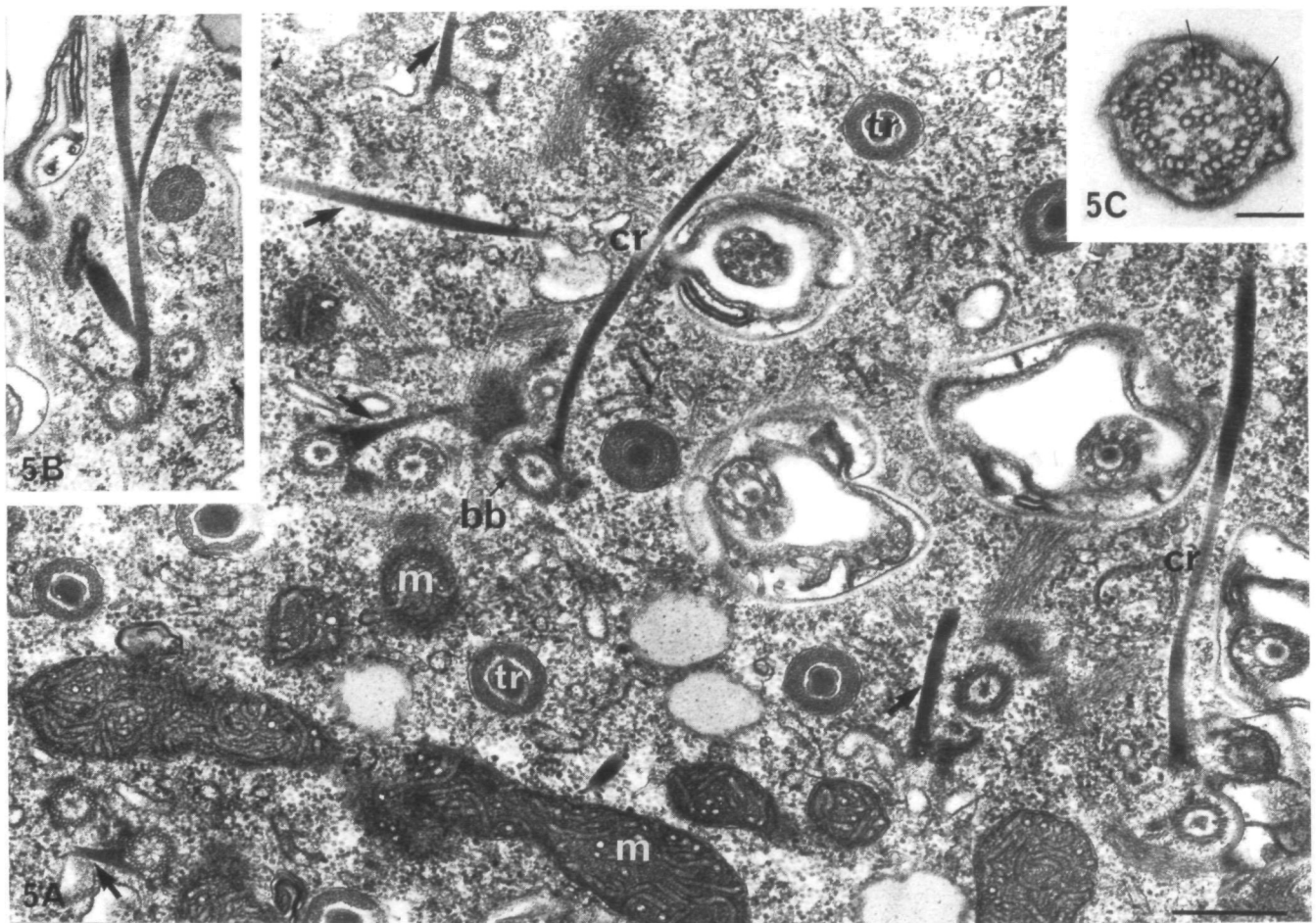


Fig. 5. Thin sections through interphase *kin241* cells. (A) The ciliary rootlets (cr) are oriented in various directions (arrows). The anterior of the cell is on the right hand side of the picture. (B) Ciliary rootlet showing a highly abnormal, forked structure. (C) Cross section through a ciliary axoneme showing additional microtubules (small arrows). bb, basal body; m, mitochondria; tr, trichocyst tip; A,B $\times 30000$, bar, $0.5\ \mu\text{m}$, C $\times 90000$; bar, $0.1\ \mu\text{m}$.

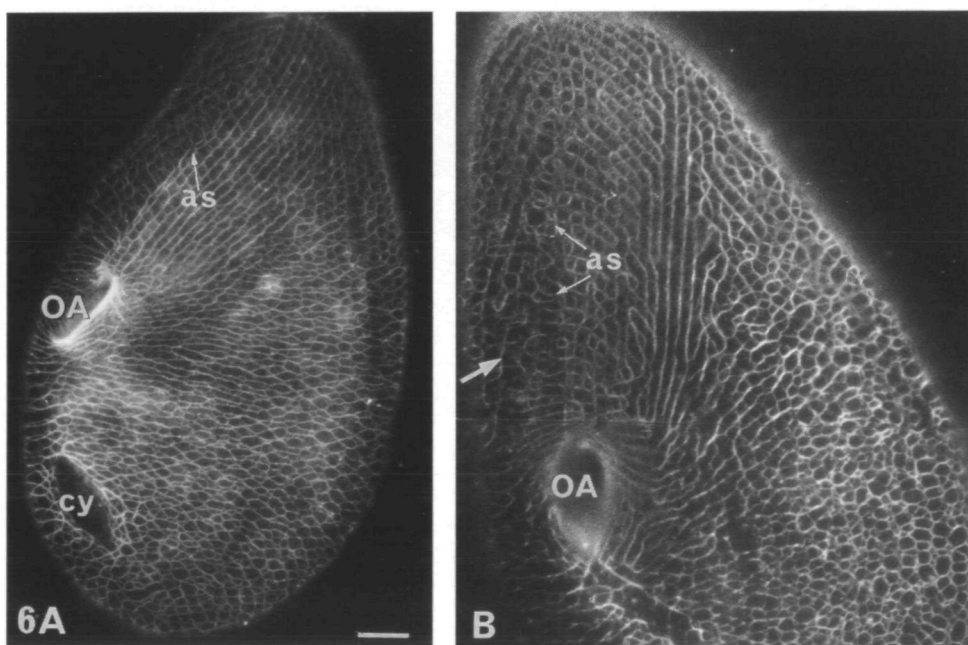


Fig. 6. Visualization of the infraciliary lattice in wild-type (A) and *kin241* (B) cells. In the mutant, the polygonal meshes of the lattice appear much more irregular both in shape and thickness. The general pattern is particularly altered along the anterior suture (as) and on its right (arrow). cy, cytoproct; OA, oral apparatus. $\times 680$; bar, $10\ \mu\text{m}$.

Table 1. Interphase cortical organization, quantitative data

	Cell size (μm)		No. of ciliary structures						Contractile vacuole pores			
	L	W	1	2	3	4	5	6	1	2	3	
WT	Range	106-123	52-66	70-76	3007-3500	4120-4651	1032-1122	215-270	482-540	2-5	136-157°	20°
	Mean	110.6 \pm 6.5	57.2 \pm 4.9	71.0 \pm 2.0	3253.3 \pm 160.0	4357.9	1105.5 \pm 35.1	247.5 \pm 24.4	497.5 \pm 20.6	2.7 \pm 1.3		
	n	8	8	8	8	8	8	8	8	9		
<i>kin24</i> new	Range	135-168	86-105	71-82	2926-3977	3735-5101	809-1138	171-230	300-561	2-6	126-157°	31°
	Mean	151 \pm 11.7	92.6 \pm 6.7	76.8 \pm 3.3	3297.1 \pm 380.5	4404.1 \pm 547	1087.5 \pm 218.3	203.6 \pm 26.32	470.6 \pm 97.8	4.1 \pm 1.5		
	n	7	7	7	7	7	7	6	6	7		
<i>kin241</i> establish	Range	186-195	112-138	80-85	4534-5254	5478-6242	892-1219	103-273	468-609	4-13	126-169°	40°
	Mean	190.3 \pm 4.1	128.5 \pm 10	82.1 \pm 1.8	4937.3 \pm 293.8	5919.5 \pm 262	1023.8 \pm 126.3	197.5 \pm 68.5	517.2 \pm 57.4	7.5 \pm 3.5		
	n	6	6	6	6	6	6	6	6	5	6	

All data concerning wt cells except those concerning contractile vacuole pores (CVP) were recalculated from Table 1 of Iftode et al (1989) Data on mutants were tallied on magnified pictures of cells labeled with antitubulin antibody *kin241* cells from new lines were studied 25-33 fissions after autogamy Established *kin241* were reisolated from the stock and grown at 27°C The following data were recorded from left to right length (L) and width (W) in μm (the width is overestimated due to severe cell compression under the coverslip), the number of (1) ciliary rows, (2) cortical units, (3) all basal bodies, (4) 2-bb units, (5) 2-bb units in right anterior field, (6) 2-bb units in left anterior field Two sources of errors are likely some basal bodies (and cus) located at the edges of the cell may be missed and there can be small ambiguities in defining the limits of terriorones containing only 1-bb or 2-bb Units were recorded to be of the 2bb type only when two basal bodies were clearly visible, thus there may be a small underestimation of 2-bb units The possible errors in counts do not exceed a few percent.

The CVPs were mapped on ciliary rows, their number (1), the angular position of the CVP sector (2), and the arcs of CVP sector (3) were calculated

All data concerning wt cells except those concerning contractile vacuole pores (CVP) were recalculated from Table 1 of Iftode et al. (1989). Data on mutants were tallied on magnified pictures of cells labeled with antitubulin antibody *kin241* cells from new lines were studied 25-33 fissions after autogamy. Established *kin241* were reisolated from the stock and grown at 27°C. The following data were recorded from left to right: length (L) and width (W) in μm (the width is overestimated due to severe cell compression under the coverslip), the number of (1) ciliary rows, (2) cortical units, (3) all basal bodies, (4) 2-bb units, (5) 2-bb units in right anterior field, (6) 2-bb units in left anterior field. Two sources of errors are likely: some basal bodies (and cus) located at the edges of the cell may be missed and there can be small ambiguities in defining the limits of territories containing only 1-bb or 2-bb. Units were recorded to be of the 2bb type only when two basal bodies were clearly visible; thus there may be a small underestimation of 2-bb units. The possible errors in counts do not exceed a few percent.

The CVPs were mapped on ciliary rows, their number (1), the angular position of the CVP sector (2), and the arcs of CVP sector (3) were calculated.

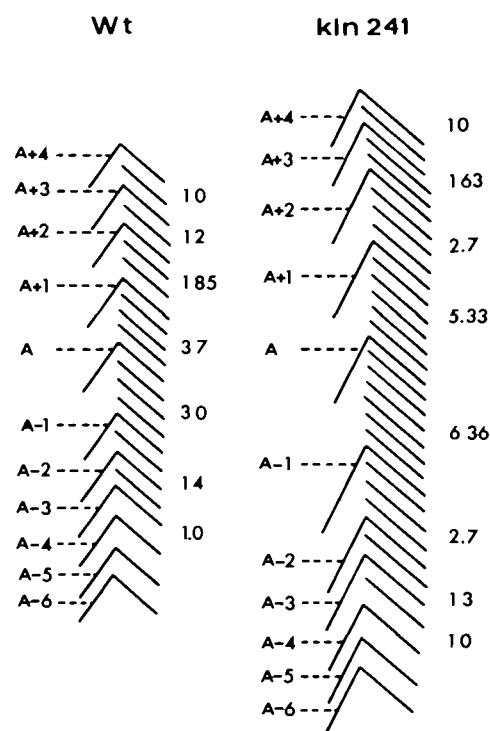


Fig. 7. Arrangement of ciliary rows around the anterior suture. The organization was compared in 7 wild-type and 19 established mutant cells labelled with antitubulin antibodies. In wild type, 11 rows from right meet 23 rows from the left of the suture. In the mutant, 11 rows from the right meet 32 rows from the left. Right rows are labelled A-6 to A+4. Row A, which can be easily identified on Fig. 1C, is defined in wild type as the one separated from both its anterior and posterior neighboring rows by the largest and almost equal number of left rows. In most cells, A is the 7th one counting from the oral apparatus. For both wt and *kin241*, the mean number of left rows within each interval between right rows is indicated to the right of the scheme. It can be noted that, contrary to wild type, *kin241* cells have more left rows posterior than anterior to A.

the cell and eventually forms a continuous array from pole to pole. While in the posterior half-cell the wave of basal body duplication spreads normally down to the posterior invariant zone and around the pole, a striking abnormality occurs in the anterior half-cell. In addition to the equatorial belt, another region of basal body proliferation is seen as an anterior subapical belt posterior to the 4-5 most anterior cus. As shown in Figs 8 and 9, on the right ventral side, this apical belt is in continuity with the equatorial zone of basal body proliferation, while on the left ventral side, it ends at the boundary of the 'invariant' field (a sector of the cortex in which no basal body duplication occurs, see Iftode et al., 1989). This abnormality is correlated with a delayed progression of the wave of basal body duplication from the equator towards the anterior pole. In this subapical zone, basal body proliferation is accompanied by cytoskeleton assembly (Fig. 9A, B) and by regression and regrowth of ciliary rootlets (not

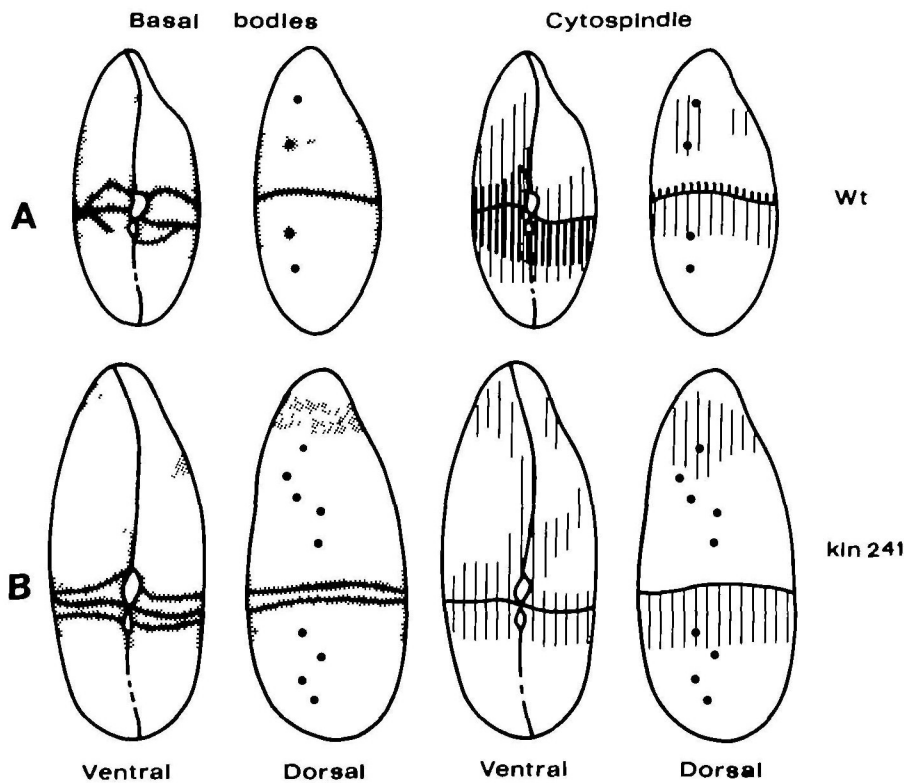


Fig. 8. Map of basal body duplication and cytoskeleton assembly at early stages of division. (A) The contours of the wave of reorganization in wild type are redrawn from Fig. 13 of Iftode et al. (1989) and correspond to stage D3. The dotted sectors visualize the first wave of basal body duplication and the solid lines delimit the progression of the second round of basal body duplication. The thick equatorial line represents the fission furrow. The black dots on the dorsal surface correspond to the contractile vacuole pores. To the right, the vertical lines indicate the state of assembly of the cytoskeleton: thick lines, continuous microtubule bundles; thin lines, discontinuous bundles. (B) In the mutant at the same stage, the second round of bb duplication is delayed whereas a subapical zone of bb proliferation and cytoskeleton assembly is present.

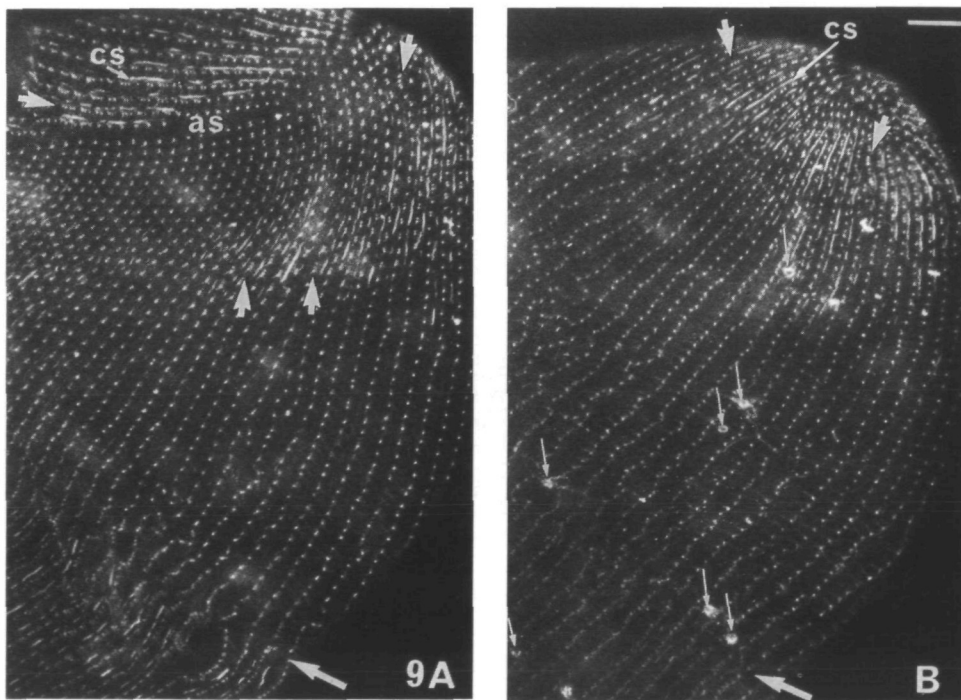


Fig. 9. Equatorial and subapical basal body multiplication in a dividing *kin241* cell. On the ventral (A) and dorsal (B) sides of a cell, at stage D3, stained with anti-tubulin antibodies, files of duplicated basal bodies are visible in units near the fission furrow (large arrow) and around the pole (short arrows). The cytoskeleton (cs) appears as short segments in the proliferating zones but has not yet developed anterior to the fission furrow. Note the number and dispersion of the contractile vacuole pores (small arrows). $\times 750$; bar, $10\ \mu\text{m}$

shown), which normally (in wild type) follow basal body duplication (Sperling et al., 1991; Fernandez-Galiano, 1978). This indicates that it is neither the nature of the response of *cus* to the morphogenetic signals nor the nature of these signals which is impaired,

but either the propagation of the signals or the competence of *cus* to respond to them.

The pattern of basal body and unit multiplication is also altered. First, overproduction of basal bodies takes place in the regions where two rounds of duplication

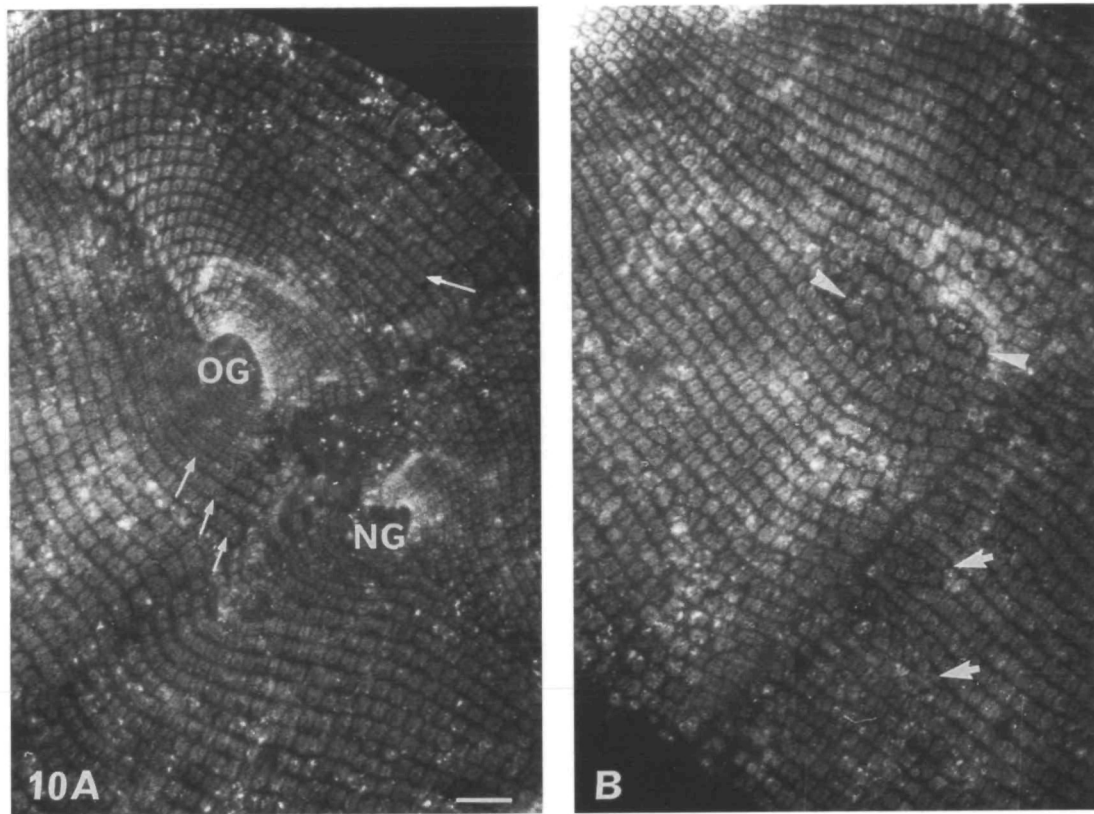


Fig. 10. Erratic unit proliferation in a dividing *kin241* cell decorated with anti-epiplasm antibodies. On both ventral (A) and dorsal (B) sides, the major abnormalities consist of files of 5 epiplasmic scales originating from a single cortical unit (arrows), patches of intercalated erratic units (arrowheads) and files of small irregular scales intercalated between pre-existing rows (short arrows). NG, new gullet; OG, old gullet. $\times 750$; bar, $10\ \mu\text{m}$.

occur during the 'first wave', essentially within an equatorial belt (Fig. 8). This is manifested by formation of files of more than 4 bbs (see Fig. 14A). Segmentation of epiplasmic scales soon yields files of 5 or more units (Fig. 10A, arrows). However, the epiplasmic scales elongate less than in wild type, and fewer will become 2-bb units during the 'second wave' of bb duplication. In addition, one domain present in wild type cells is grossly reduced in the mutant (see Fig. 11A), the domain posterior to the left anterior 'invariant' field, composed of 2-bb units which present a unique mode of duplication with elongation of the epiplasmic scale preceding basal body duplication (see Iftode et al. 1989). Altogether, these observations are consistent with the data of Table 1 which show that *kin241* cells possess an excess of 1-bb units (approximately 1.5 times the number in wild type) but no more 2-bb units than wild type. It therefore appears that *kin241* cells undergo an enhanced first wave and a reduced second wave of bb duplication.

Most likely correlated with overduplication of basal bodies during the first wave, insertion of units (or files of units) between pre-existing rows is observed (Fig. 10 A, B), a process which may either generate additional rows and/or create the disorders observed in particular in the right anterior field (Figs 2A, 4A).

The difference between wild type and mutant in the extent and localization of basal body and unit duplication is summarized in Fig. 11. It appears that the overall excess of basal body and unit proliferation results from (a) a reduction in zone 2, (b) a modification of the properties of zone 1 accompanied by some extension of its surface and (c) the appearance of zone 6, an additional zone of hyperproliferation.

Finally, a most intriguing abnormality was the formation of an ectopic secondary fission break. This break initially appears as a gap between epiplasmic scales as does the normal fission furrow. It was most often found on the right dorsal side in posterior division products, possibly originating as a fork from the main furrow, spanning 8-25 ciliary rows. It starts at about 3-5 units (in early dividers) and about 13 units (in late dividers) and ends about 10-20 units posterior to the fission furrow (Fig. 12 A, B).

In early dividers, basal body proliferation similar to that around the normal furrow was seen, yielding packed basal bodies and a bending of the rows anterior to the break (Fig. 12A, B). Remnants of the break are visible in interphase cells as a 'scar' marked by disordered basal bodies and ciliary rootlets and irregular epiplasmic scales (Fig. 4C). In cells displaying the ectopic furrow, cytokinesis was sometimes impaired,

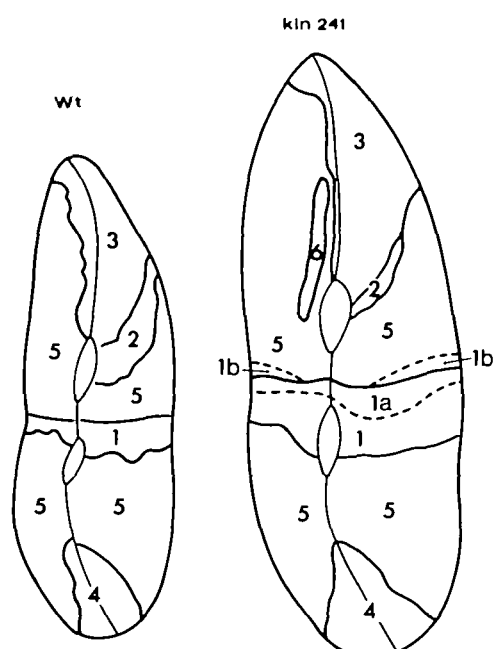
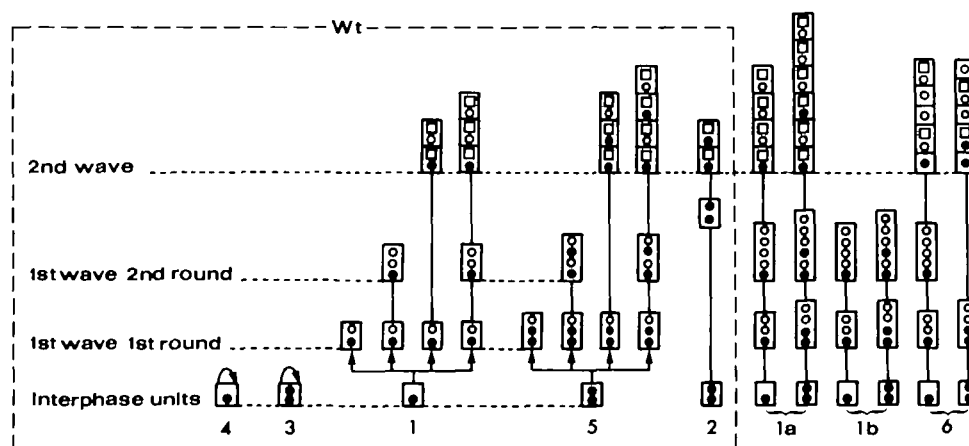


Fig. 11. Regionalized patterns of basal body and cortical unit duplication in wt and *kin241* cells at stage D-4 of division. The WT pattern is taken from Fig. 7C and 7D of Iftode et al. (1989). In zone 1, one or two rounds of bb duplication have taken place and the second wave is in progress. In zone 5, only the first wave of bb duplication has taken place. In zones 3 and 4 the basal bodies do not duplicate at all. In zone 2, the old bbs in 2-bb units move apart before generating a new bb. In *kin241*, in zones 1 and 5, two subdomains (1a, 1b) of hyperpoliferation are present. In zone 6, which does not exist in wild type, there is hyperduplication. Finally the area of zone 2 is reduced. The different patterns of bb duplication in WT (boxed in figure) and *kin241* are summarized in the lower part. From bottom to top, the scheme depicts the chronology of addition of new basal bodies (open circles for first wave addition, open squares for second wave addition) from interphase 1-bb or 2-bb units, depending on their location in either one of the zones 1-5. Aside from basal bodies in invariant 1-bb or 2-bb units (in zones 4 and 3 in which no bb duplication occurs) and from the zone 2 basal bodies only involved in a second wave of duplication, all parental units undergo either one or two rounds of basal body duplication in the first wave, followed or not by a second wave of duplication. In *kin241* cells, additional patterns of duplication occur: 1a: hyperduplication followed by a second wave. 1b: hyperduplication without second wave. 6: hyperduplication with or without second round.



yielding chains of unseparated daughter cells. The secondary break was more frequently observed in young clones than in established ones.

(B) Alterations in the organization of cortical structures

Basal bodies duplicate like centrioles by budding of a neoformed organelle perpendicular to the mother structure. As described by Dippell (1968), the new basal body originates from a germinative disc precisely located anterior to the mother basal body, and the neoformed cylinder tilts up and reaches the cell surface anterior and parallel to the old one (Fig. 13A). This leads to the precise intercalation of new basal bodies along the preexisting ciliary rows. Therefore, at least in ciliates, basal body duplication obeys a polarity constraint which is an autonomous property of the cortical unit, independent of the overall cell polarity (Beisson and Sonneborn, 1965). Abnormal localizations of newly formed bbs with respect to the mother one were

observed in thin sections of the mutant (Fig. 14B, C). As shown in Fig. 13B, those abnormal duplications account for the mispositioning of new basal bodies.

Abnormalities in the assembly of ciliary rootlets were observed in some dividing cells with two crs in a single cortical unit, forming a V-shaped structure (Fig. 15A). At the E.M. level, the second cr appeared to be nucleated either on the left anterior side (Fig. 15C) or on the posterior part of the basal body (Fig. 15D). The secondary cr assembled near the microtubule triplet N°1 points posteriorly, while the crs nucleated near triplets 5-6 run toward the anterior left. Double crs were observed in both 1-bb or 2-bb units (Fig. 15B and D respectively), in the latter case on the posterior basal body. In wild-type cells, in 2-bb units, the single cr is nucleated on the posterior basal body.

Finally, abnormal organization of the basal bodies themselves were observed with extra microtubules in either the external triplets or within the lumen of the basal body (Figs 5C, 14D).

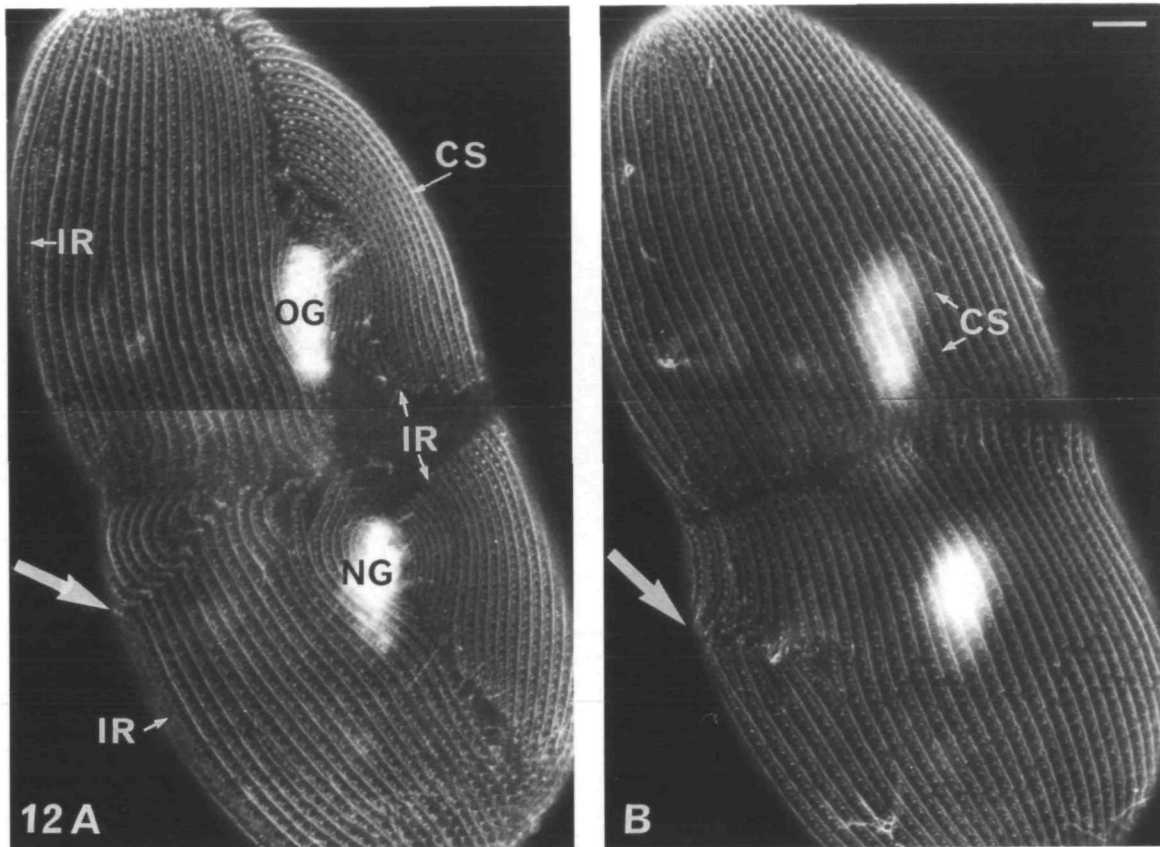


Fig. 12. Ventral (A) and dorsal (B) aspects of a dividing *kin241* cell from a new line 35 divisions old showing the secondary fission break (thick arrow) and inverted rows (IR) of basal bodies. The cytospindle (CS) is continuous throughout the cell. The cell was immunostained with the anti-tubulin antibodies. NG, new gullet; OG, old gullet. $\times 680$; bar, $10\ \mu\text{m}$.

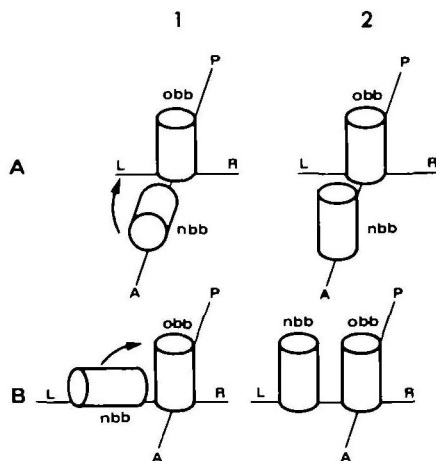


Fig. 13. Normal (A) and modified (B) orientation of newly formed bb (nbb) with respect to the mother bb (obb). A, P and L, R respectively represent the body axes.

Discussion

The mutation *kin241* is characterized by its dual effects on cortical unit organization and global cortical pattern and by its variable expression. The various abnormalities described here are neither all found in every cell,

nor equally pronounced in all cells. Furthermore, the phenotypic analysis is complicated by the fact that cortical disorders can be perpetuated or amplified through successive divisions. Therefore one needs (1) to sort out which of the morphological defects are 'primary', i.e. do not result from previous disorders and (2) to consider only the qualitative nature of the defects, regardless of the extent or frequency of their expression. As interphase organization is the end-result of the morphogenetic processes of division, we shall first consider the anomalies recorded during division and the extent to which they can account for the interphase phenotype, then discuss at which level the mutation is likely to act.

(1) Morphogenetic defects

At the cortical unit level, the most striking defect is the occurrence of newly formed basal bodies which develop at an abnormal site and consequently do not position anterior to the mother basal body. Since previous data (Beisson and Sonneborn, 1965; Dippell, 1968) have established that in wild-type cells, the polarity of each basal body (and hence the organization of each cortical unit) is an autonomous property independent of the whole cell polarity, it therefore seems that the mutation *kin241* affects the properties (polarity, nucleation activity) of the basal body or of its close environment.

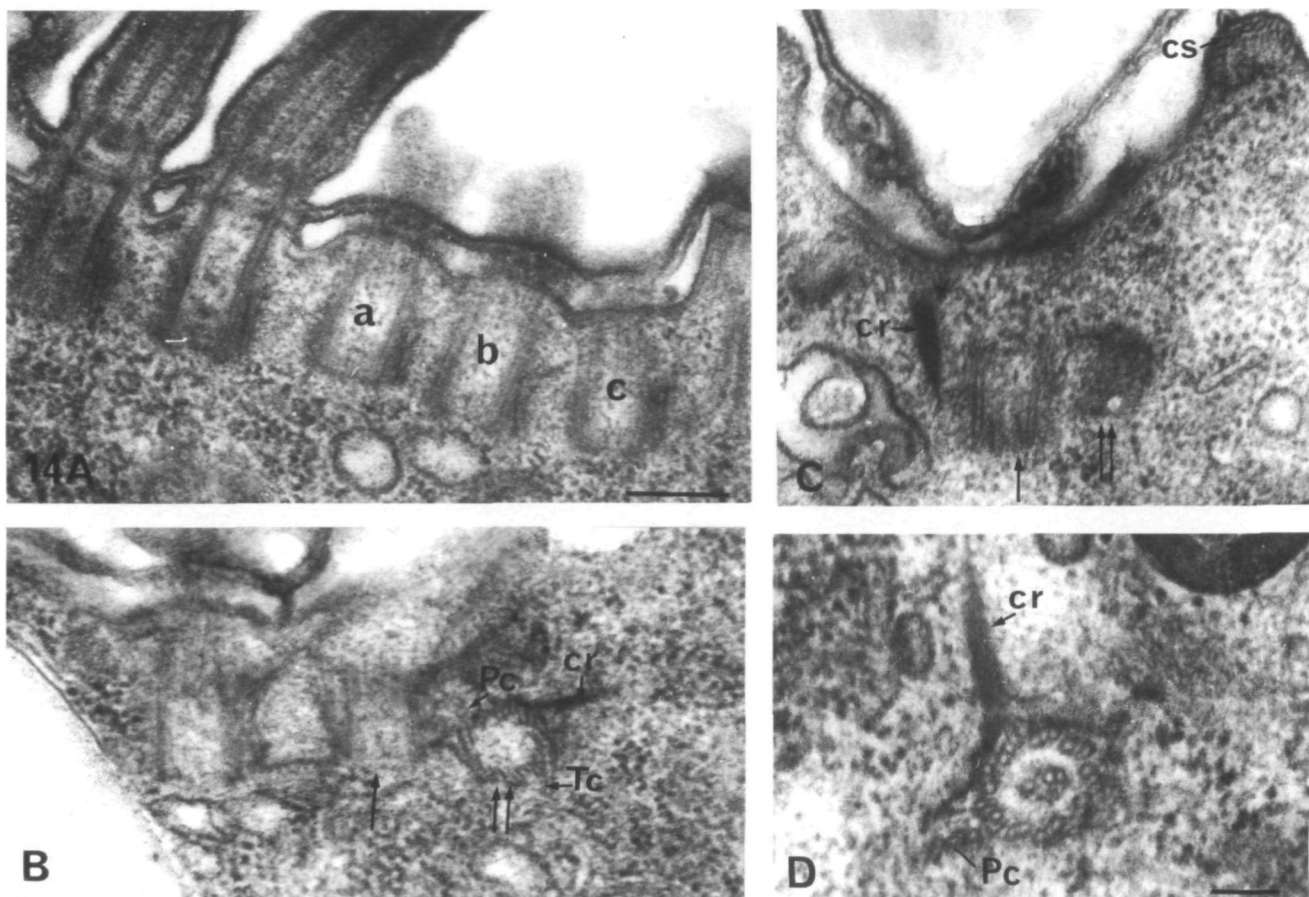


Fig. 14. Sections through dividing *kin241* cells. (A) The anterior of the cell on A and B is on the right-hand side of the micrograph. Three newly formed basal bodies (a,b,c) anterior to the 2 old ones from a 2bb unit. (B) A young basal body (double arrow) in abnormal orientation with respect to its mother (arrow). It is perpendicular to the old bb, but faces it not by cartwheel structure, but by the blade of triplet N°1. Note that the new basal body possesses cr, Pc and Tc ribbons. (C) The anterior of the cell is in front of the viewer. Longitudinal section through a developed basal body (arrow) and a nascent one (double arrow). The new bb is assembled on the cell's left side of the preceding one instead of anteriorly. (D) A basal body from the mid-dorsal surface of the posterior division product. In the lumen of the basal body, three microtubules are visible. The accessory structures, Pc and cr, are normal. cs, cytospinde. A, B, C $\times 65000$; bar, $0.2 \mu\text{m}$. D $\times 90000$; bar, $0.1 \mu\text{m}$.

This conclusion is supported by the various other defects observed: occurrence of a secondary ciliary rootlet and of occasional extra microtubules in the basal body itself, abnormal shapes of some cortical units and excess or mislocalization of parasomal sacs (although the mechanism of localization of parasomal sacs relative to other components of the cortical units is unknown).

At the whole cell level, the modifications of the spatiotemporal program of unit proliferation include: (1) enhanced first wave (with hyperproliferation of basal bodies more pronounced in the anterior half-cell) and reduced second wave of duplication; (2) modified progression of the morphogenetic waves in the anterior half-cell; (3) occasional appearance of an ectopic fission furrow. However, wherever basal bodies and units proliferate, be it at abnormal times or places, unit duplication per se shows a normal coordination of basal body duplication, epiplasmic scale fragmentation, regression and regrowth of the ciliary rootlets. It then can be concluded that the mutation affects neither the

nature of the morphogenetic signal(s), nor the competence of the structures to respond to the signals. Most probably, the mutation also does not affect the nature of the structural proteins. The analysis of wild-type development has shown the existence of some sort of positional information endowing different precisely delimited cortical domains each with the capacity to respond in its own way to the morphogenetic signals. For instance (see Fig. 11), field 3 is invariant, fields 1 and 5 are highly proliferative, field 2 undergoes a single round of basal body duplication during the second wave. The structural or biochemical basis of this regionalization remains to be discovered, but is most likely related to the setting of the anteroposterior/and circumferential gradients. In the mutant, the variability from cell to cell and the modified spatiotemporal map of morphogenetic processes indicate that the properties of the domains are less well fixed and/or that the contours of the domains are less well defined. This might explain in particular the ectopic secondary fission furrow, the

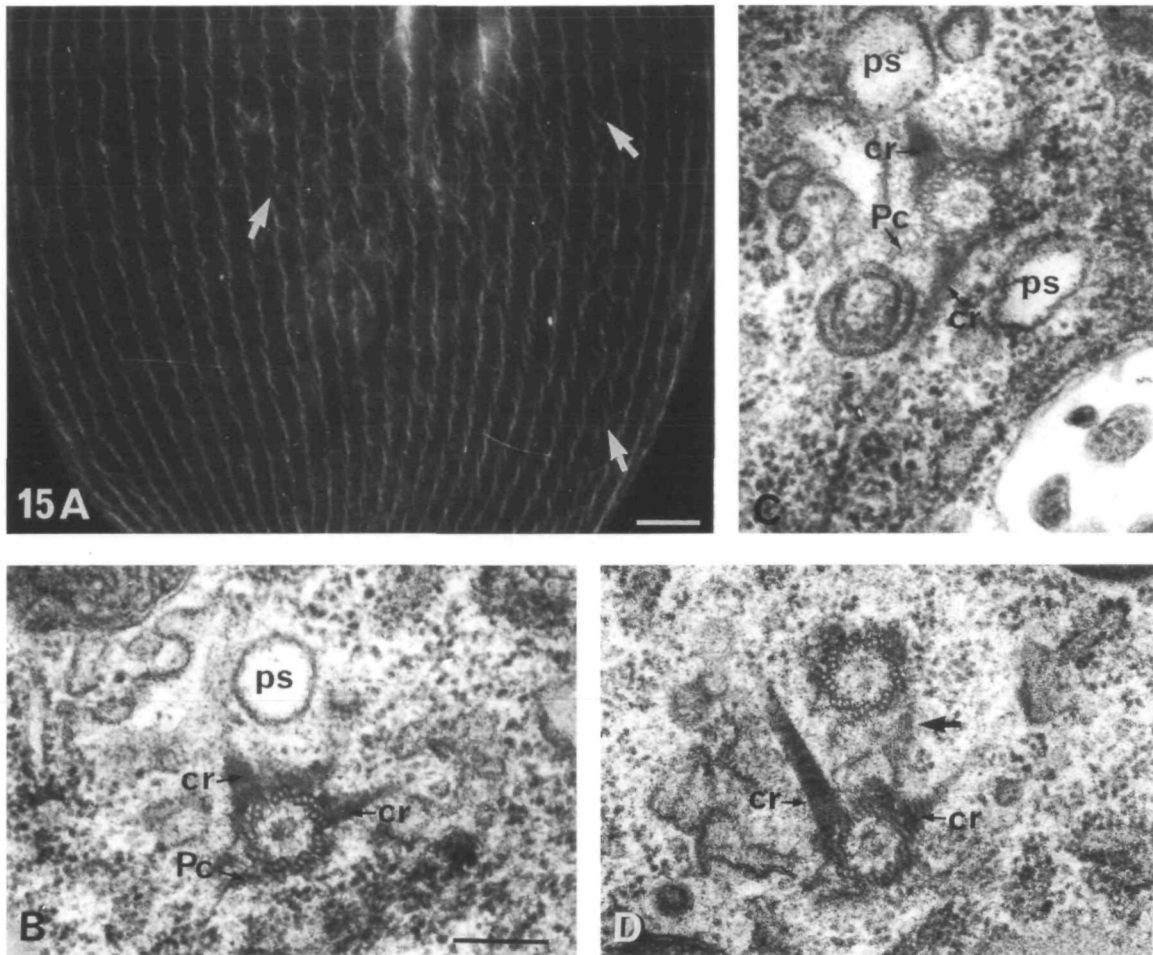


Fig. 15. Duplicated striated ciliary rootlets (cr). (A) The dorsal side of young *kin241* post-dividing cell 3 divisions after autogamy immunostained with the anti-cr antibodies. Many V-shaped crs are present, some are indicated by arrows. (B, C, D) Cross sections show bb of late dividing *kin241* cell. (B) Two cr fibers are visible: on right (normal) and left (additional) sides of the bb. The additional cr is attached to microtubular triplets 3 and 4 and points anterior-left of the cell. A parasomal sac (ps) is visible between the two crs. (C) A basal body with two striated fibers (cr). The secondary one is attached to triplets 1 and 2 and points posterior. Note also the modified location of the parasomal sacs (ps). (D) 2-bb unit in which the posterior bb bears two crs and a bridge structure (arrow) joining it to the anterior bb. A $\times 750$; bar, 10 μm . B, C, D $\times 60000$; bar, 0.2 μm .

delay in the anterior propagation of the first wave of basal body duplication, the reduction of field 2, and the generation of more contractile vacuole pores over a larger sector of the cell circumference.

(2) From defective morphogenesis to the interphase phenotype

A most conspicuous trait of *kin241* cells is their large size. However, it is clear that the *kin241* mutation is not a large cell size mutation. The study of 'new' mutant lines shows that the size characteristic of 'established' lines is acquired progressively and rather slowly. Then a steady state is reached, which may depend on the capacity of the biosynthetic machinery and correspond to the upper limit of the stability range of the corticotype as discussed by Frankel (1980). The progressive increase in cell size, number of ciliary rows and cortical units and the correlative appearance of cortical

disorders can all be accounted for by the enhanced first wave of basal body proliferation and mislocalization of some newly formed basal bodies (see Fig. 10). The combined effects of these abnormalities suffices to generate new rows, more units of smaller size within each row, as well as disordered patches of units (with cortical units of bizarre shapes and ciliary rootlets pointing in various directions), and IRs from 180° rotated basal bodies.

However, the defects in pattern are not randomly located: the most extensive ones are along the anterior suture (see Figs 2A, 4A) which derives from the fission furrow of the previous division, that is from the zone of hyperproliferation of basal bodies and cortical units. The generation of disorders on the right contrasts with the ordered rows on the left. This difference may be related to the fact that the development of the posterior daughter cells involves (at least, in wild type) more surface elongation on the right than on the left.

Table 2. Mutations affecting basal body duplication, orientation and associated structures

		Phenotype							
Species	Gene	Basal bodies			Associated structures		Axoneme		References
		Duplication	Orientation	Structure	Striated fibers	Microtubular ribbons	Structure	Growth	
<i>Chlamydomonas</i>	<i>bld-2</i>	<	+	+	—	—	+	+	Goodenough and St Clair, 1975
	<i>uni-1</i>	<	—	—	—	—	+	+	Huang et al 1982
	<i>uni-2</i>	<					+	+	
	<i>uni-3</i>	<					+	+	
	<i>vfl-1</i>	>	+	+	+	+	+	+	Adams et al 1985
	<i>vfl-2</i>	>	+	—	+				Wright et al 1985
									Jarvik and Suhan 1991
	<i>vfl-3</i>	>	+	—	+	+		+	Wright et al 1983
<i>Paramecium</i>	<i>sm-19</i>	<	—	+	—	—	+	—	Ruiz et al 1987
	<i>kin-241</i>	>	+	+	+		+		Jerka-Dziadosz et al this paper

Based on the works cited in reference, + indicates that the phenotypic trait is altered, — that it is not altered and a blank indicates that the information is not available. In the column 'Duplication', > stands for overduplication and < for hypoduplication.

As for the localization of IRs, they prevail on the right half of the cell circumference in two sectors: near the ventral suture and at the CVP meridian. In young clones they are formed also near the left side of the anterior suture. In wild-type cells, IRs generated on the right side of the oral apparatus have been shown to slowly move around the cell over many cell generations (Beisson and Sonneborn, 1965). To account for this 'cortical slippage' in *Paramecium*, also described in *Tetrahymena* by Nanney (1967), a mechanism has recently been proposed (Iftode and Adoutte, 1991) which involves generation, at division, of new bb rows on the right edge of the oral apparatus in the anterior fission product and loss of basal body rows on the left edge of the OA in the posterior division product. In *kin241* cells, IRs do not seem to progress beyond the zone of CVPs. This arrest may be due to a defect in the mechanism of cortical slippage proposed by Iftode and Adoutte (1991). In addition, it can be related to the broadening of the CVP domain and destabilization of domain boundaries. In other mutants in which broadening of cortical domains occurs, namely the *bcd* mutant of *Tetrahymena* (Cole et al., 1987) and the *mlm* mutants of *Paraurostyla* (Jerka-Dziadosz and Wiernicka, 1992), misorientation of ciliary structures results in anteroposteriorly reversed oral membranelles and ciliary structures at the borders of the broadened domains. According to the Cyclic Instability Model (Jerka-Dziadosz, 1989) based on general premises of the Cylindrical Coordinate Model proposed by Frankel (1989, 1990), the likely destabilization of positional values, resulting in an intercalation of values in reversed order to restore the continuity around the cell circumference, would generate, or at least stabilize, cortical patches of reversed polarity in addition to broadening some domains. This interpretation, although highly speculative, accounts for the restricted localization of the IR and the broadening of the CVP and left to ventral ciliary row domains (Fig. 7). All

other defects observed in interphase *kin241* cells can be directly accounted for by the abnormalities recorded at division at both cortical unit and whole cell levels. However, a major question concerns the causal relationships between the two levels of defects.

(3) Possible relationships between local and global effects of the mutation

Even at the cortical unit level, the effects of the mutations are varied. In order to discuss the possible relationships between these local defects and those disturbing the global pattern, one first needs to examine whether the different local abnormalities (in positioning of new bbs, ciliary rootlet nucleation, bb ultrastructure) are likely to be independently determined. It is then of interest to compare *kin241* with other mutations affecting basal bodies. As shown in Table 2, among 9 mutations studied in *Chlamydomonas* and *Paramecium*, 6 affect basal body duplication and all 6 also disturb at least one (*sm19*) or several other properties such as orientation, ultrastructure or associated structures. The pleiotropy at the cortical unit level of the mutation *kin241* is therefore not exceptional and the effects of these various mutations suggest a tight coupling between the duplication of basal bodies, their structure and their organizational capacity, which can all be ascribed to a single local defect.

Three types of causal relationships between local and global effects can then be envisaged: (1) the mutation affects some basal body property and this defect causes large scale defects; (2) the mutation affects the control of global patterning and this results in the observed local defects; (3) the mutation affects some upstream factor which indirectly or directly controls processes at both levels.

In the first hypothesis, a primary defect in basal body positioning can directly account for the qualitative abnormalities of the global pattern, but the hyperproliferation of basal bodies and abnormal deployment of

the morphogenetic wave would require an additional assumption. The modified responses of the cortical domains to the morphogenetic wave would result from defects in basal body and unit duplication. This is unlikely since, at least in wild type, the properties of the domains are conferred by their localization on the surface: cortical units, whose lineage can be followed (Iftode et al., 1989), show no intrinsic or transmissible properties, as their progeny may occupy different domains and behave according to the domain where they are located. Nothing supports the conclusion that transmissible properties of particular cortical units exist in the mutant.

In the second hypothesis, an initial defect in cell polarity and delimitation of the cortical domains might reduce the accuracy of basal body duplication and generate the qualitative cortical defects. However, this is unlikely because the mutation *kin241* is exceptional by its dual effects on basal body properties and on global pattern. Various mutations studied in ciliates alter the global pattern: the *bcd1*, *bcd2* and the *janus* mutations in *Tetrahymena* (Cole et al., 1987; Frankel and Nelsen, 1986; Jerka-Dziadosz, 1981) or the *mlm* and *pl* mutations in *Paraurostyla* (Jerka-Dziadosz, 1989; Jerka-Dziadosz and Wiernicka, 1992): none of them alter basal body or cortical unit characteristics. Conversely, two other mutants, *sm19* in *Paramecium* (Ruiz et al., 1987), and *bbs* in *Euplotes* (Frankel, 1973), which cause underduplication of basal bodies and both underduplication and misorientation of basal bodies, do not affect global pattern, although in the latter case the fidelity of cytoplasmic inheritance of preexisting row number was considerably reduced. Although these examples do not rule out that some alterations in the control of global pattern might cause defects at the cortical unit level, they rather argue against a primary defect on the control of global pattern.

Finally in the third hypothesis, both local and global defects would be simultaneously caused by a change in some physiological parameter. In support of this hypothesis which seems to us to be the most likely, it is important to consider that the data reported here document only one aspect of the effects of the *kin241* mutation, which also affects non-cortical developmental processes, namely nuclear reorganization. In wild-type cells, after conjugation or autogamy, the zygotic nucleus undergoes two successive mitoses and the sister nuclei issued from the second postzygotic division differentiate into either micronuclei or macronuclei according to their respective brief positioning at the anterior or posterior cell pole (Grandchamp and Beisson, 1981). This reveals differential determinative properties of the two polar regions most likely correlated with a gradient of internal Ca^{2+} concentration (Grandchamp and Beisson, unpublished data). In *kin241*, the zygotic nucleus generally undergoes one more post-zygotic division, yielding 8 nuclei. However, in contrast to what is observed in another mutant, *mic44*, which regularly forms 4 micronuclei (m) and 4 macronuclei (M) (Grandchamp and Beisson, 1981), nuclear reorganization in *kin241* cells yields a range of

combinations from 0m:8M to 8m:0M. These abnormalities do not seem to be correlated with defective elongation of the separation spindles of the third postzygotic division but rather suggest an abnormal and quite variable localization from cell to cell of the determinative properties of the subcortical endoplasm (Rossignol, Grandchamp and Beisson, unpublished data). A significant repair of these abnormalities is obtained in the presence of 2×10^{-4} M EDTA applied 1-2 divisions before induction of nuclear reorganization (Beisson et al., 1976; Rossignol and Beisson, unpublished data). The effect of EDTA on cortical organization was not studied because of the difficulty of quantifying cortical defects and the lethal effect of EDTA during prolonged exposure. Altogether, it is likely that the mutation affects the generation of Ca^{2+} gradients in or near the cortex during nuclear reorganization and division. A model based upon generation of Ca^{2+} waves has been proposed to account for the morphogenetic waves in *Paramecium* (Le Guyader and Hyver, 1990; 1991). The generation of Ca^{2+} waves might rely on the Ca^{2+} -sensitive mechanoreceptors whose polarized distribution in the plasma membrane has been demonstrated (Ogura and Machemer, 1980). Precisely localized Ca^{2+} release (or Ca^{2+} induced Ca^{2+} release) might also arise from the subpellicular alveoli, a submembranar Ca^{2+} store (Stelly et al., 1990) closely apposed to the outermost cytoskeletal networks. Furthermore, recent data on the teratogenic effect of Li^+ on *Paramecium* have led to postulate the existence of gradients of activity of the polyphosphatidylinositol (PI) cycle and a role of spatially graded liberation of secondary messengers (Ca^{2+}) in the control of morphogenetic processes (Beisson and Ruiz, 1992). In conclusion, it is striking that both the particularities of nuclear reorganization and the analysis of the cortical disorders independently suggest that the *kin241* mutation disturbs the geography of cortical differentiation. As previously pointed out, the mutation does not alter either the nature of the morphogenetic signals nor the capacity of the cortical cytoskeleton to respond to the signals. One is then led to conclude that the mutational defect lies in a defective spatial control of either the generation or the transduction of the signals within the cortex. A defective distribution of the mechanoreceptors or of other, PI associated, surface receptors involved in spatially modulated Ca^{2+} release might account for the various effects of the mutation and is in principle accessible to experimental demonstration.

(4) The mutation *kin241* and the dissection of morphogenetic processes

What does the study of the *kin241* mutation reveal about the interplay of local constraints and interactions within the cortical unit, propagation of the transcellular signals and interpretation of the signals according to the cortical domain or the nature of the signal(s) and the molecular or structural basis of domain differentiation?

A most striking phenotypic trait of the *kin241* cells concerns the modification not only of the boundaries but also of the properties (expressed in particular in

new patterns of basal body and unit proliferation as shown in Fig. 11) of some domains. The correlated change in the limits and the properties of domains confirms that a domain corresponds to a structural or biochemical differentiation of the cortex which controls the response to the morphogenetic signals. As previously pointed out, the mutation does not alter either the nature of the morphogenetic signal(s) or the capacity of cortical units to respond, but only their local interpretation. The hypothesis that the geography of the domains is related to the distribution of the mechanoreceptors is attractive and testable.

The other interesting feature of the *kin241* phenotype concerns the abnormal positioning of some basal bodies and the correlated disorders in ciliary rootlet nucleation and in cortical unit shape and alignment. It is clear from the cytological data that the errors in the positioning of new basal bodies appear as a rather rare event and are not perpetuated in the lineage of the mispositioned basal bodies. This indicates that the geometry of basal body and cortical unit duplication, although constrained within the preexisting unit organization, also depends on other global physiological parameters.

We thank Drs J. Frankel, A. Adoutte and L. Sperling for critical reading of the manuscript. The work was supported by grants from the Centre National de la Recherche Scientifique, the 'Ligue Nationale Française contre le Cancer' and the 'Fondation pour la Recherche Médicale'. M. Jerka-Dziadosz benefited from grants from the Polish Academy of Science and a CNRS 'poste rouge' for visiting scientists. The technical help from Mrs. Lidia Wiernicka is kindly acknowledged.

References

- Adams, W., Wright, R. L. and Jarvik, J. W. (1985) Defective temporal and spatial control of flagellar assembly in a mutant of *Chlamydomonas reinhardtii* with variable flagellar number. *J Cell Biol* **100**, 955-964.
- Allen, R. D. (1971) Fine structure of membranous and microfibrillar systems in the cortex of *Paramecium caudatum*. *J. Cell Biol* **49**, 1-20.
- Bailly, E., Berges, J., Bordes, N., Celati, C. and Bornens, M. (1988) Analysis of centrosomal components with monoclonal antibodies. *Europ Symp on the Struct. Funct. Cytoskeleton* Lyon, France Abstr 87, p 143.
- Beisson, J., Rossignol, M., Ruiz, F., Adoutte, A. and Grandchamp, S. (1976) Genetic analysis of morphogenetic process in *Paramecium*. a mutation affecting cortical pattern and nuclear organization (Abstr) *J Protozool* **23**, 3A.
- Beisson, J. and Ruiz, F. (1992). Lithium-induced respecification of pattern in *Paramecium*. *Dev Genet* (In press).
- Beisson, J. and Sonneborn, T. M. (1965) Cytoplasmic inheritance of the organization of the cell cortex of *Paramecium aurelia*. *Proc Natl Acad Sci U S A* **53**, 275-282.
- Bornens, M., Paintrand, M., Berges, J., Marty, M. C. and Karsenti, E. (1987). Structural and chemical characterization of isolated centrosomes. *Cell Motil Cytosk* **8**, 238-249.
- Cohen, J., Adoutte, A., Grandchamp, S., Houdebine, L. M. and Beisson, J. (1982) Immunochemical study of microtubular structures throughout the cell cycle of *Paramecium*. *Biol Cell* **44**, 35-44.
- Cole, E. S., Frankel, J. and Jenkins, L. M. (1987) *bcd*. mutation affecting the width of organelle domains in the cortex of *Tetrahymena thermophila*. *Roux's Arch. Dev Biol* **196**, 421-433.
- Dippell, R. W. (1968). The development of basal bodies in *Paramecium*. *Proc Natl Acad Sci U S A* **61**, 461-468.
- Ehret, C. F. and McArdle, E. W. (1974) The structure of *Paramecium* as viewed from its constituent levels of organization. In *Paramecium: A current Survey* (ed W. J. Van Wagtenonk) pp 263-338. Amsterdam: Elsevier.
- Fernandez-Galliano, D. (1978) Le comportement des cinétosomes pendant la division de *Paramecium caudatum*. *Protistologica* **14**, 291-294.
- Frankel, J. (1973) A genetically determined abnormality in the number and arrangement of basal bodies in a ciliate. *Dev Biol* **30**, 336-365.
- Frankel, J. (1980). Propagation of cortical differences in *Tetrahymena*. *Genetics* **94**, 607-623.
- Frankel, J. (1989) *Pattern Formation: Ciliate Studies and Models*. Oxford University Press, New York.
- Frankel, J. (1990) Positional order and cellular handedness. *J Cell Sci* **97**, 205-211.
- Frankel, J. and Nelsen, E. M. (1986) How the mirror-image pattern specified by a *janus* mutation of *Tetrahymena* comes to expression. *Dev Gen* **6**, 213-238.
- Fukushi, T. and Hiwatashi, K. (1970) Preparation of mating reactive cilia from *Paramecium caudatum* by $MnCl_2$. *J Protozool* **17** (Suppl.) Abstr 21.
- Garreau de Loubresse, N., Keryer, G., Vigues, B. and Beisson, J. (1988) A contractile cytoskeletal network of *Paramecium*, the infraciliary lattice. *J Cell Sci* **90**, 351-364.
- Garreau de Loubresse, N., Klotz, C., Vigues, B., Rutin, J. and Beisson, J. (1991) Ca^{2+} -binding proteins and contractility of the infraciliary lattice in *Paramecium*. *Biol Cell* **71**, 217-225.
- Goodenough, W. W. and St Clair, H. S. (1975) Bald-2: a mutation affecting the formation of doublet and triplet sets of microtubules in *Chlamydomonas reinhardtii*. *J Cell Biol* **66**, 480-491.
- Grandchamp, S. and Beisson, J. (1981) Positional control of nuclear differentiation in *Paramecium*. *Dev Biol* **81**, 336-341.
- Huang, B., Ramanis, S. Z., Dutcher, S. K. and Luck, D. J. L. (1982) Uniflagellar mutants of *Chlamydomonas*: evidence for the role of basal bodies in the transmission of positional information. *Cell* **29**, 745-753.
- Iftode, F. and Adoutte, A. (1991). Un mécanisme de régulation morphogénétique chez *Paramecium*: la rotation du cortex. *C. R. Hebd Seanc Acad Sci Paris Vol 313, Série III*, 65-72.
- Iftode, F., Cohen, J., Ruiz, F., Torres Rueda, A., Chen-Shan, L., Adoutte, A. and Beisson, J. (1989) Development of surface pattern during division in *Paramecium*. I Mapping of duplication and reorganization of cortical cytoskeletal structures in the wild-type. *Development* **105**, 191-211.
- Jarvik, J. W. and Suhan, J. P. (1991) The role of the flagellar transition region: inferences from the analysis of a *Chlamydomonas* mutant with defective transition region structure. *J Cell Sci* **99**, 731-740.
- Jerka-Dziadosz, M. (1981) Patterning of ciliary structures in *janus* mutant of *Tetrahymena* with mirror-image cortical duplications. An ultrastructural study. *Acta Protozool* **20**, 337-356.
- Jerka-Dziadosz, M. (1989). Defective spatial control in patterning of microtubular structures in mutants of the ciliate *Paraurostyla*. II Spatial coordinates in a double recessive mutant. *Eur J Protistol* **24**, 323-335.
- Jerka-Dziadosz, M. and Beisson, J. (1990) Genetic approaches in ciliate pattern formation: From self-assembly to morphogenesis. *Trends Genet.* **6**, 41-45.
- Jerka-Dziadosz, M. and Wiernicka, L. (1992) Ultrastructural studies on development of cortical structures in the ciliary pattern mutants of the hypotrich ciliate *Paraurostyla weissii*. *Europ J Protistol* (in press).
- Keryer, G., Adoutte, A., Ng, S. F., Cohen, J., Garreau de Loubresse, N., Rossignol, M., Stelly, M. and Beisson, J. (1990) Purification of the surface membrane-cytoskeleton complex (cortex) of *Paramecium* and identification of several of its protein constituents. *Europ J Protistol* **25**, 209-225.
- Le Guyader, H. and Hyver, C. (1990) Modeling of the duplication of cortical units along a kinetic of *Paramecium* using reaction-diffusion equations. *J Theor Biol* **143**, 233-250.
- Le Guyader, H. and Hyver, C. (1991). Duplication of cortical units on the cortex of *Paramecium*: A model involving a Ca^{2+} wave. *J Theor Biol* **150**, 261-276.

- Nanney, D. L. (1967) Cortical slippage in *Tetrahymena* *J Exp Zool* **166**, 163-170.
- Ogura, A. and Machemer, H. (1980) Distribution of mechanoreceptor channels in the *Paramecium* surface membrane *J. Comp Physiol.* **135**, 233-242.
- Ruiz, F., Garreau de Loubresse, N. and Beisson, J. (1987) A mutation affecting basal body duplication and cell shape in *Paramecium* *J Cell Biol* **104**, 417-430
- Schliwa, M. and Van Blerkom, J. (1981). Structural interactions of cytoskeletal components *J Cell Biol* **90**, 222-235.
- Sonneborn, T. M. (1970) Gene action in development *Proc Roy Soc Lond.* **176**, 347-366
- Sonneborn, T. M. (1974). *Paramecium aurelia*. In: *Handbook of Genetics* III (ed R C King), pp 469-594 New York. Plenum.
- Sonneborn, T. M. (1975). Positional information and nearest neighbour interactions in relation to spatial patterns in ciliates *Ann Biol.* **XIV**, 565-584
- Sperling, L., Keryer, G., Ruiz, F. and Beisson, J. (1991). Cortical morphogenesis in *Paramecium* a transcellular wave of protein phosphorylation involved in ciliary rootlet disassembly. *Dev Biol* **148**, 205-218
- Stelly, N., Mauger, J. P., Claret, M. and Adoutte, A. (1991) Cortical alveoli of *Paramecium*. a vast submembranous calcium storage compartment *J Cell Biol* **113**, 103-112
- Viguès, B. and Grolère, C. A. (1985) Evidence for a Ca^{2+} -binding protein associated to non-actin microfilamentous systems in two ciliated protozoans *Expl Cell Res* **159**, 366-376
- Wright, R. L., Chojnacki, B. and Jarvik, J. W. (1983) Abnormal basal body number, location and orientation in a striated fiber-defective mutant of *Chlamydomonas reinhardtii* *J. Cell Biol.* **96**, 1697-1707
- Wright, R. L., Salisbury, J. and Jarvik, J. W. (1985) A nucleus basal body connector in *Chlamydomonas reinhardtii* that may function in basal body localization or segregation *J Cell Biol* **101**, 1903-1912

(Accepted 2 March 1992)